Title

The Importance of the Pseudomonas aeruginosa Type III Secretion System in Epithelium Traversal Depends upon Conditions of Host Susceptibility

Journal

Infection and Immunity, 83(4)

ISSN

0019-9567

Authors

Sullivan, Aaron B
Tam, KP Connie
Metruccio, Matteo ME
et al.

Publication Date

2015-04-01

DOI

10.1128/iai.02329-14

Peer reviewed

IAI Journals.ASM.org

The Importance of the *Pseudomonas aeruginosa* Type III Secretion System in Epithelium Traversal Depends upon Conditions of Host Susceptibility

Aaron B. Sullivan,[a] K. P. Connie Tam,[a]* Matteo M. E. Metruccio,[a] David J. Evans,[a,b] Suzanne M. J. Fleiszig[a,b,c]

School of Optometry, University of California, Berkeley, California, USA[a]; College of Pharmacy, Touro University California, Vallejo, California, USA[b]; Graduate Groups in Vision Science, Microbiology, and Infectious Diseases and Immunity, University of California, Berkeley, California, USA[c]

***Pseudomonas aeruginosa* is invasive or cytotoxic to host cells, depending on the type III secretion system (T3SS) effectors encoded. While the T3SS is known to be involved in disease *in vivo*, how it participates remains to be clarified. Here, mouse models of superficial epithelial injury (tissue paper blotting with EGTA treatment) and immunocompromise (MyD88 deficiency) were used to study the contribution of the T3SS transcriptional activator ExsA to epithelial traversal. Corneas of excised eyeballs were inoculated with green fluorescent protein (GFP)-expressing PAO1 or isogenic *exsA* mutants for 6 h *ex vivo* before bacterial traversal and epithelial thickness were quantified by using imaging. In the blotting-EGTA model, *exsA* mutants were defective in capacity for traversal. Accordingly, an ~16-fold variability in *exsA* expression among PAO1 isolates from three sources correlated with epithelial loss. In contrast, MyD88$^{-/-}$ epithelia remained susceptible to *P. aeruginosa* traversal despite *exsA* mutation. Epithelial lysates from MyD88$^{-/-}$ mice had reduced antimicrobial activity compared to those from wild-type mice with and without prior antigen challenge, particularly 30- to 100-kDa fractions, for which mass spectrometry revealed multiple differences, including (i) lower baseline levels of histones, tubulin, and lumican and (ii) reduced glutathione *S*-transferase, annexin, and dermatopontin, after antigen challenge. Thus, the importance of ExsA in epithelial traversal by invasive *P. aeruginosa* depends on the compromise enabling susceptibility, suggesting that strategies for preventing infection will need to extend beyond targeting the T3SS. The data also highlight the importance of mimicking conditions allowing susceptibility in animal models and the need to monitor variability among bacterial isolates from different sources, even for the same strain.**

Pseudomonas aeruginosa remains a leading cause of respiratory infections, septicemia, and urinary tract and burn wound infections (1–4). It is also the most common cause of corneal infection associated with contact lens wear (5, 6). Our research has shown that clinical and laboratory isolates of *P. aeruginosa* can be divided into invasive or cytotoxic strains based upon how they interact with host cells (7). Invasive strains can survive and replicate inside epithelial cells dependent on the type III secretion system (T3SS) effector ExoS (8–10), while cytotoxic strains instead encode ExoU, which can induce rapid death of intoxicated host cells (11, 12). While details of how invasive and cytotoxic strains impact host cells vary, both types can cause human disease, and they can each be virulent in animal models of infection (13–15).

Several *in vivo* models exist for studying *P. aeruginosa* pathogenicity. They include *Caenorhabditis elegans* (16–18) and *Drosophila melanogaster* (19), in addition to mouse models of pneumonia with sepsis (20–22), burn wound infection with sepsis (23–25), and gastrointestinal colonization and sepsis (26, 27) and corneal scarification models (28–30). Despite this plethora of available host models, the mechanisms by which *P. aeruginosa* (and other microbes) traverse barriers *in vivo* to cause infection remain poorly understood, probably because the principles upon which most are based necessitate deliberately bypassing them to initiate the disease to be studied. For example, the corneal scarification model involves scratching through both the corneal epithelium and the basal lamina of mouse corneas to allow bacteria direct access to the underlying corneal stroma, an event required for triggering of visible corneal pathology (keratitis). Consequently, the model is well suited to studying what occurs after bacteria have gained access into the corneal stroma, and much has been learned through its utilization for that purpose (31–35). Indeed, we have used it to show that the T3SS can participate in keratitis caused by *P. aeruginosa* (28, 30, 36). However, the scarification model cannot be used to study how bacteria traverse the corneal epithelium, an earlier step bypassed by the scratching process. It is important to study epithelial traversal, given that contact lens-related infection is not usually preceded by stromal exposure, and lens wear is the most common predisposing factor for corneal infection caused by *P. aeruginosa*.

Other investigators have used monolayers of various cell types to study epithelial cell traversal by *P. aeruginosa* and have shown roles for proteases, exotoxin A, multidrug resistance efflux pumps, and the T3SS (27, 37–39). Indeed, the ADPr activity of

Received 14 July 2014 **Returned for modification** 18 August 2014
Accepted 30 January 2015

Accepted manuscript posted online 9 February 2015

Citation Sullivan AB, Tam KPC, Metruccio MME, Evans DJ, Fleiszig SMJ. 2015. The importance of the *Pseudomonas aeruginosa* type III secretion system in epithelium traversal depends upon conditions of host susceptibility. Infect Immun 83:1629–1640. doi:10.1128/IAI.02329-14.

Editor: B. A. McCormick

Address correspondence to Suzanne M. J. Fleiszig, fleiszig@berkeley.edu.

* Present address: K. P. Connie Tam, Cole Eye Institute, Cleveland Clinic, Cleveland, Ohio, USA.

Supplemental material for this article may be found at http://dx.doi.org/10.1128/IAI.02329-14.

doi:10.1128/IAI.02329-14

ExoS, one of the T3SS effectors, has been found to disrupt epithelial tight junctions and facilitate paracellular bacterial localization (37). To more closely mimic *in vivo* corneal epithelium, our laboratory has instead used corneal epithelial cells grown as multilayers, and using them has revealed roles for proteases, pilus-mediated twitching motility, and the T3SS (40–42). However, traversal of a multilayered epithelium that has formed on the surface of an actual cornea (or other tissue) in the context of other factors present *in vivo* could be a different task for the bacteria than traversing a monolayer grown *in vitro*. Indeed, in previous studies we reported that exposure of cultured epithelial cells to mucosal (tear) fluid protected against bacterial virulence, a phenomenon that endured after the mucosal fluid was removed (43). This, and changes to gene expression in the mucosal fluid treated epithelial cells, revealed that the mechanism for protection involved lasting changes to the state of the epithelial cell once exposed to mucosal fluid and that it involved specific microRNAs (43, 44).

Several years ago, we described a method for studying bacterium-epithelium interactions *in vivo* that was a modification of the scarification model. The idea was based on our observations that 6 h after scratching, corneas remained susceptible to infection despite the fact that healing epithelium visibly covered the stroma. We used this "6-h healing" model to study the role of ExsA, a transcriptional activator for the *P. aeruginosa* T3SS (45), in enabling keratitis while epithelial cells covered the stroma. Both PAO1 (invasive) and PA103 (cytotoxic) could cause keratitis in this model, but ExsA influenced colonization and entry into the stroma for only the cytotoxic strain. While this suggested that ExsA was dispensable for bacteria to traverse the healing corneal epithelium in the case of the invasive strain, several caveats need to be considered. The first is that the bacteria entered the stroma, showing that the basal lamina barrier between the epithelium and stroma (41), not only the epithelial barrier, remained compromised at the 6-h time point. Indeed, the speed and number of bacteria entering the stroma showed that compromise of both "barriers" was severe. Second, the study was carried out more than a decade ago, when we lacked methods for accurately localizing bacteria within the epithelium and were limited to studying (and extrapolating from) representative thin sections. Thus, there might have been differences we could not detect. Further, we performed the bacterial inoculation step *in vivo*, so host factors, such as eyelids, blinking, and tear fluid, could have influenced the outcome beyond their role in modulating epithelial defenses.

More recently, we developed a suite of *in vivo* and *ex vivo* models to allow early steps in pathogenesis to be studied, requiring no or minimal injury to the epithelium (46, 47). We have also advanced our imaging methods and analysis software to allow accurate localization/quantification of all bacteria in corneas of live eyeballs, without need for fixation or sectioning (47). Our published data obtained using these models suggest that multiple levels of defense protect the healthy cornea. They show that uninjured normal mouse ocular surfaces rapidly cleared *P. aeruginosa*, even when enormous inocula ($>10^{11}$/ml) were applied (48, 49), contrasting scratch injury, after which the corneas succumb to destructive keratitis with 6 to 8 orders of magnitude fewer bacteria (28, 30, 31, 50). We showed that blotting the corneal surface with tissue paper (Kimwipe), which disrupts tight junctions while otherwise leaving corneas morphologically similar, made corneas susceptible to bacterial adhesion without subsequent epithelial traversal. When blotting was followed by 1 h of EGTA treatment (100 mM in phosphate-buffered saline [PBS]), the bacteria could traverse the epithelium all the way to the underlying basal lamina (46). Using gene knockout mice, we have found that MyD88 is important for protecting the corneal epithelium against both adhesion and subsequent traversal (47) and that mBD3, the mouse equivalent of human hBD2 and a MyD88-dependent factor (51, 52), is involved in this protective effect (49). We further showed that these novel methods for studying traversal of *in situ*-grown corneal epithelium could be adapted for *ex vivo* use, which allows exclusion of tear fluid and infiltrating phagocytic responses when desirable.

Here, we examined the role of ExsA in invasive *P. aeruginosa* traversal of the corneal epithelium using these new models of superficial injury (blotting plus EGTA) and immunocompromise ($MyD88^{-/-}$), which both make the epithelium permissive to traversal while retaining the basal lamina barrier (46, 47), and outcomes were assessed using our new imaging methods (47). This was done using PAO1, an invasive strain that traverses the corneal epithelium to the level of the basal lamina in both models, and *ex vivo* conditions to exclude direct effects of tear fluid, blinking, and other extracorneal factors during bacterial inoculation (46, 47).

MATERIALS AND METHODS

Bacteria. *P. aeruginosa* strain PAO1 encodes three known T3SS effectors: ExoS, ExoT, and ExoY. Three different sources of wild-type PAO1 were used. PAO1 source A was used by us previously in our *in vivo* and *ex vivo* studies of *P. aeruginosa* traversal of murine corneal epithelia (46, 47). PAO1 source B was used as the parent of the isogenic *exsA* mutant (PAO1exsA::Ω) that cannot transcriptionally activate the T3SS (53). PAO1 source C was included for additional comparison of T3SS expression *in vitro* and traversal *ex vivo* in both models. For imaging, all bacteria, including the *exsA* mutant, were complemented (by electroporation) with plasmid pSMC2 encoding green fluorescent protein (GFP) and grown on Trypticase soy agar (TSA) supplemented with 300 μg/ml carbenicillin overnight (~18 h) at 37°C. The *exsA* mutant of PAO1 source B was complemented with pEB124 kindly provided by Timothy Yahr, University of Iowa (54). For use in experiments, bacteria were resuspended in serum-free tissue culture medium (Dulbecco's modified Eagle medium [DMEM]; Gibco) without antibiotics to a concentration of ~10^{11} CFU/ml, confirmed by viable count. Plasmid-complemented strains grew equally well *in vitro* (data not shown).

P. aeruginosa strain 6206 was used for testing the antimicrobial activity of corneal cell lysates. TSA-grown bacteria (~18 h, 37°C) were resuspended in serum-free keratinocyte basal medium (KBM) (Lonza, Inc.) to a concentration of ~10^8 CFU/ml (absorbance of 0.1 at 650 nm) and then diluted in sterile water or lysate fractions to a final concentration of 10^6 CFU/ml for use in experiments.

***Ex vivo* murine models of *P. aeruginosa* epithelial traversal.** All procedures were approved by the Animal Care and Use Committee of the University of California, Berkeley. Wild-type C57BL/6 mice (6 to 8 weeks old) or MyD88 gene knockout ($MyD88^{-/-}$) mice of the same strain and age were used for all experiments. All experiments were performed *ex vivo*. Thus, after sacrifice, eyes were enucleated, rinsed three times with PBS, and placed in a 96-well tissue culture plate (Corning). Eyes were incubated at 37°C (5% CO_2) or for microscopy in a chamber slide with a water-jacketed heater set to 37°C. For each model described below, each experimental group contained 4 to 8 eyes.

For experimental model 1 (tissue paper blotting plus EGTA treatment), eyes of wild-type mice were blotted with a Kimwipe (Kimtech) before incubation in EGTA (100 mM in PBS) for 1 h at 37°C. Eyes were then rinsed three more times in PBS, transferred to bacterial suspension, and then incubated for 6 h. After bacterial exposure, eyes were rinsed with PBS to remove nonadherent bacteria, affixed to a glass coverslip with

cornea facing up, and submerged in Ham's F-12 medium (Lonza) for imaging.

For experimental model 2, eyes from C57BL/6 MyD88$^{-/-}$ mice were used. The mice were kindly provided by Greg Barton (University of California, Berkeley) and bred in our facilities. These eyes were not blotted or EGTA treated, but following three rinses with PBS, they were placed in bacterial suspension for 6 h. After bacterial exposure, eyes were rinsed with PBS to remove nonadherent bacteria, affixed to a glass coverslip with the cornea facing up, and submerged in Ham's F-12 medium (Lonza) for imaging.

Imaging of murine eyes by confocal and 2-photon microscopy. The imaging method used was previously described (47). Briefly, eyes were imaged using a Zeiss LSM 510 NLO META Axioplan confocal and 2-photon microscope equipped with a Spectra-Physics MaiTai HP DeepSee laser for 2-photon imaging (700 to 1,020 nm), and 458-nm, 488-nm, 514-nm, 543-nm, and 633-nm laser lines (Molecular Imaging Center, University of California, Berkeley). W Plan-Apochromat (63×/1.0, M27; working distance [WD] = 2.1 mm) and Achroplan IR (40×/0.80, W; WD = 3.6 mm) dipping objectives were used. A 720-nm laser was used to visualize autofluorescence of NADPH inside live cells. Corneal cells were also imaged without chemical fixing and labeling by using a 633-nm laser to obtain reflection of all cells (live or dead). For each eye, optical slices were taken at 0.5-μm intervals from the apical surface of the corneal epithelial cells (if present) through the entire thickness of the epithelium and into the anterior stroma (to an ~50-μm depth). Reconstruction of three-dimensional (3D) and transverse images for each sample was done using imaging software described previously (47).

Measurement of corneal epithelial thickness and bacterial traversal. Corneal thickness was measured using the Zeiss LSM imaging software. Reflectance and autofluorescence confocal overlaid images were divided into a 3-by-3 grid, and the thickness of the epithelium was measured using measurement tools provided within the software package. At least 9 measurements were averaged across 4 to 8 corneas per test group, and means and standard deviations were calculated. Bacterial traversal was measured as previously described (47). In some instances, a lack of epithelial uniformity required an alternate method for measuring epithelial thickness and bacterial traversal. Briefly, 3D models of epithelial surfaces and bacteria were generated using IMARIS (Bitpane, South Windsor, CT), and distances between the epithelial surfaces and bacteria were computed using a distance transformation via a MATLAB (Mathworks Torrance, CA) plug-in within IMARIS. Distances to both the apical epithelial surface and bacteria were measured from the basal lamina to compute epithelial thickness and bacterial traversal, respectively.

RT-PCR. To determine *exsA* gene expression *in vitro*, bacteria were grown under T3SS-inducing conditions, i.e., tryptic soy broth (TSB) containing glycerol (1% [vol/vol]), monosodium glutamate (50 mM), EGTA (5 mM), and $MgCl_2$ (50 mM) (55) at 37°C, to exponential growth phase and harvested by centrifugation (~11,000 × *g*, 10 min). Non-T3SS-inducing conditions (TSB alone) were used for controls. RNA was isolated from bacteria using TRIzol (Life Technologies, Grand Island, NY). A DNase I kit (Fermentas) was used to eliminate contaminating DNA, and cDNA was made for real-time PCR (RT-PCR) using an Ambion MessageAmp II bacterial kit (Life Technologies). RT-PCR was performed on an Applied Biosystems Step One Plus (Life Technologies). Primers were designed using Applied Biosystems Primer Express software and verified by a BLAST search. Gene sequences were obtained from the *Pseudomonas* genome database (www.pseudomonas.com). RT-PCR primers were 16S rRNA for PAO1 (forward, GGCGCTAATACCGCATACGT, and reverse, TGATAGCGTGAGGTCCGAAGA) and *exsA* (forward, CATGGAGGCG GGCTTTT, and reverse, CGAAACGGCGGCGATAG). Primers were synthesized by IDT (Coralville, IA).

Antimicrobial activity assay. Whole corneas from enucleated mouse eyes were exposed to *P. aeruginosa* antigens (supernatant of *P. aeruginosa* PAO1 source B culture [56]; 5 μl/eye for 3 h) or a Trypticase soy broth control, then ground/homogenized in distilled water with micropestles, and spun at 14,000 × *g* for 2 min to remove cell debris and remaining stromal tissue. Crude lysates were confirmed to have equal total protein concentrations using a BCA (bicinchoninic acid) assay kit (Pierce Biotechnology, Inc., Thermo Scientific, Rockford, IL). Serial fractionation of crude lysates was performed at 4°C using sterile-water-prerinsed Microcon centrifugal filter devices with membrane cutoffs at 100, 30, and 10 kDa (Millipore). Fresh vehicle was added to all lysate fractions to maintain a volume equal to that of their original crude lysates. Bacteria (60 μl; 10^6 CFU/ml of suspended lawn culture of *P. aeruginosa* strain 6206) in lysate fractions or water were incubated in triplicate at 37°C for 3 h. Serial dilutions of the samples at time zero and 3 h were plated on nutrient agar plates and incubated at 37°C overnight for viable bacterial counts (CFU/ml). The percent survival at 3 h was determined as follows: (bacterial counts of lysate fraction at 3 h/bacterial counts of distilled water at 3 h) × 100%.

Mass spectrometry. Corneal lysate fractions were prepared as described above, except that corneas were ground/homogenized in 100 mM Tris-HCl (pH 8.5). Mass spectrometry was performed at the Proteomics/Mass Spectrometry Laboratory at University of California, Berkeley. A nano-liquid chromatography (nano-LC) column was packed in a 100-μm-inner-diameter glass capillary with an emitter tip. The column consisted of 10 cm of Polaris C_{18} 5-μm packing material (Varian, Lake Forest, CA). The column was loaded by use of a pressure bomb and washed extensively with buffer A (5% acetonitrile–0.02% heptafluorobutyric acid [HBFA]). The column was then directly coupled to an electrospray ionization source mounted on a Thermo-Fisher LTQ XL linear ion trap mass spectrometer. An Agilent 1200 high-performance liquid chromatograph (HPLC) equipped with a split line so as to deliver a flow rate of 30 nl/min was used for chromatography. Peptides were eluted with a 90-min gradient from 100% buffer A to 60% buffer B (80% acetonitrile–0.02% HBFA). Collision-induced dissociation (CID) and electron transfer dissociation (ETD) spectra were collected for each *m/z*. The programs SEQUEST and DTASELECT were used to identify peptides and proteins from the murine database. A minimum cutoff two different peptides was set to identify proteins, and total spectral counts from each protein were used to calculate relative abundance (57). A 2-fold difference or more was considered significant. Heat maps were generated using the CIMminer tool (http://discover.nci.nih.gov/cimminer).

Statistics. Data are expressed as the mean ± standard deviation (SD) for each sample group. Statistical significance between three or more groups was determined using analysis of variance (ANOVA) with Tukey's multiple-comparison *post hoc* analysis. Unpaired Student's *t* test was used for two-group comparisons of normally distributed data. *P* values of <0.05 were considered significant.

RESULTS

ExsA is required for invasive *P. aeruginosa* to traverse the murine corneal epithelium *ex vivo* after superficial injury. The T3SS of *P. aeruginosa* is regulated by the transcriptional activator ExsA (53, 58). To explore its role, mouse corneas were inoculated with an *exsA* mutant of *P. aeruginosa* strain PAO1 (~10^{11} CFU/ml) *ex vivo* for 6 h, and results were compared to those for corneas infected with the wild type (source B). Before inoculation, corneas were blotted and EGTA treated to enable bacterial adhesion and subsequent traversal of the corneal epithelium (46). Figure 1 shows the contrast between wild-type- and *exsA* mutant-infected corneas. Surprisingly, PAO1 source B was found to be highly destructive to the corneal epithelium and almost completely removed it from the cornea, allowing bacteria (Fig. 1A, green) to adhere directly to the basal lamina. Still, bacteria were not seen within the stroma, showing that despite the destruction/loss of epithelium, the basal lamina barrier remained competent. In contrast, the epithelium was relatively intact after exposure to the *exsA* (T3SS) mutant (Fig. 1B), with bacteria (green) adhering only to

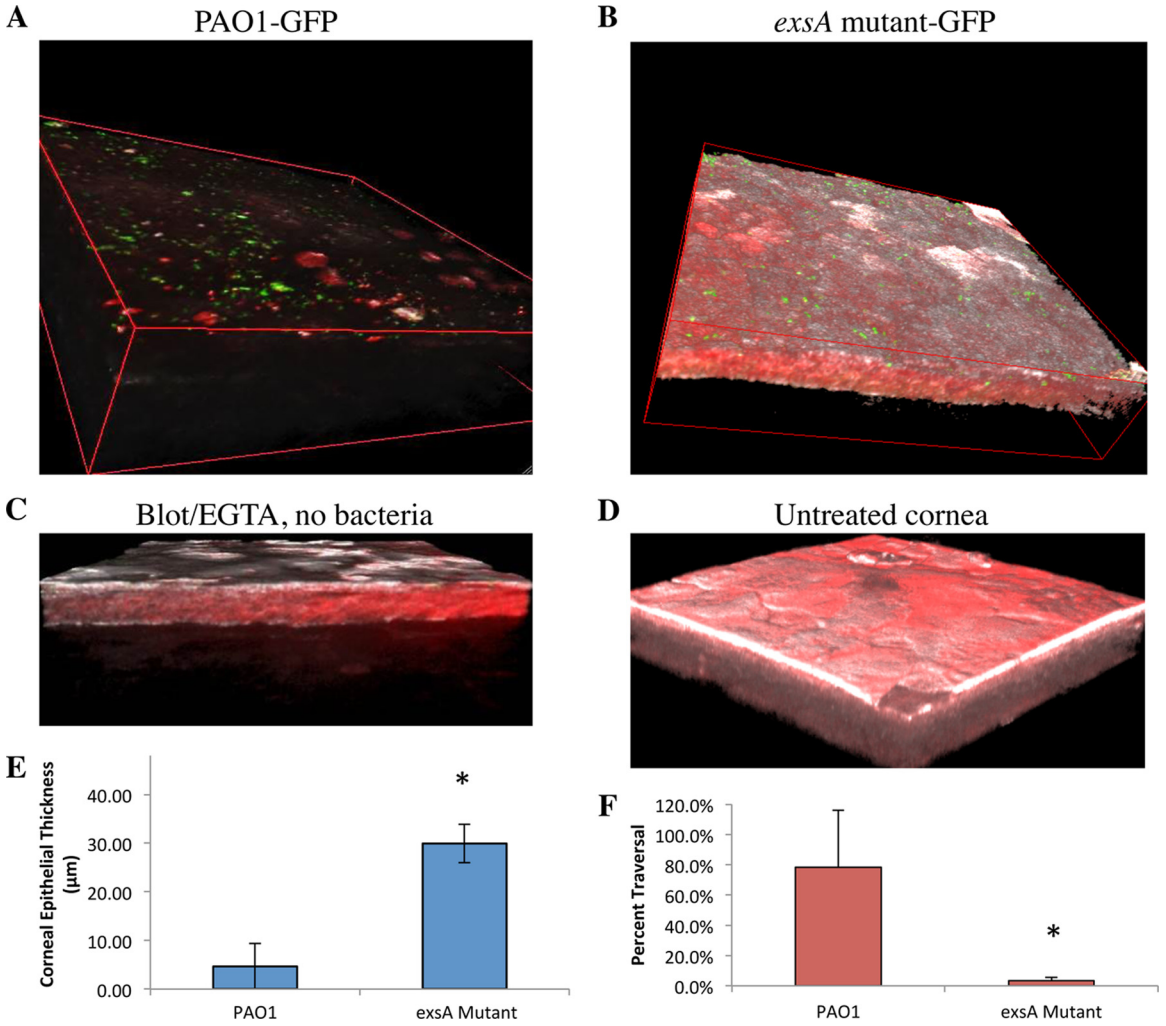

FIG 1 *P. aeruginosa* traversal of the murine corneal epithelium in the tissue paper blottting-EGTA model. In each instance, eyeballs were blotted with tissue paper and treated with EGTA (100 mM in PBS, 1 h) prior to bacterial exposure. (A) Invasive *P. aeruginosa* strain PAO1-GFP (green) source B caused significant damage to the murine corneal epithelium after 6 h exposure *ex vivo*, denoted by the absence of epithelial cell autofluorescence (red) by confocal and 2-photon microscopy. (B) In contrast, exposure to a T3SS (*exsA*) mutant (PAO1*exsA*::Ω-GFP) left the corneal epithelium relatively intact, and bacteria (green) adhered. (C) Control showing murine corneal epithelium after blotting-EGTA treatment but without bacterial inoculation. (D) Untreated murine corneal epithelium. (E) An ~6-fold difference in corneal epithelial thickness was seen after exposure to PAO1 compared to the *exsA* mutant (*, $P = 0.016$, *t* test). (F) Percent traversal of PAO1-GFP compared to PAO1*exsA*::Ω-GFP (*, $P = 0.008$, *t* test). Representative images from six independent experiments are shown. A Zeiss LSM 512 Meta W Plan-Apochromat (63×/1.0) objective lens was used. White, host cell reflectance at 633 nm.

the epithelial surface. Controls were included to confirm that the epithelium remained intact if the blotting-EGTA treatment was done without bacterial inoculation (Fig. 1C) and if the cornea was untreated, i.e., it underwent no blotting or EGTA treatment and was not exposed to bacteria (Fig. 1D). Quantification of the data collected showed that there was an ~6-fold difference in corneal epithelial thickness after exposure to wild-type PAO1 compared to its *exsA* mutant ($P = 0.016$; *t* test) (Fig. 1E). There was also a significant difference in the percentage traversal between PAO1 and its *exsA* mutant (Fig. 1F) ($P = 0.008$; *t* test).

Under experimental conditions similar to those described for Fig. 1, complementation of the *exsA* mutant of PAO1 source B with *exsA* was associated with an ~54% reduction in epithelial thickness compared to the *exsA* mutant alone (analysis of 3 eyeballs across central and peripheral corneas) ($P = 0.037$; *t* test). Controls using cultured corneal epithelial cells revealed that *exsA* complementation restored the ability of the *exsA* mutant to cause cell rounding, verifying that the T3SS was expressed and functional (data not shown).

PAO1 isolates from different sources vary in their capacity to traverse mouse corneal epithelium, and this capacity is correlated with *exsA* gene expression. The above data suggested a role for the ExsA-regulated T3SS in mediating bacterial traversal of the corneal epithelium. However, the magnitude of the epithelial damage observed with this source of PAO1 was far greater than in our published studies using PAO1-GFP source A (46, 47). Thus, PAO1-GFP source B was compared to two other isolates of PAO1 from different laboratories (see Materials and Methods) in the same assay. Three-dimensional and transverse section images show significant variations between the three sources of PAO1 (Fig. 2). PAO1 source A demonstrated behavior similar to that seen in our previous studies by binding to, and partially traversing,

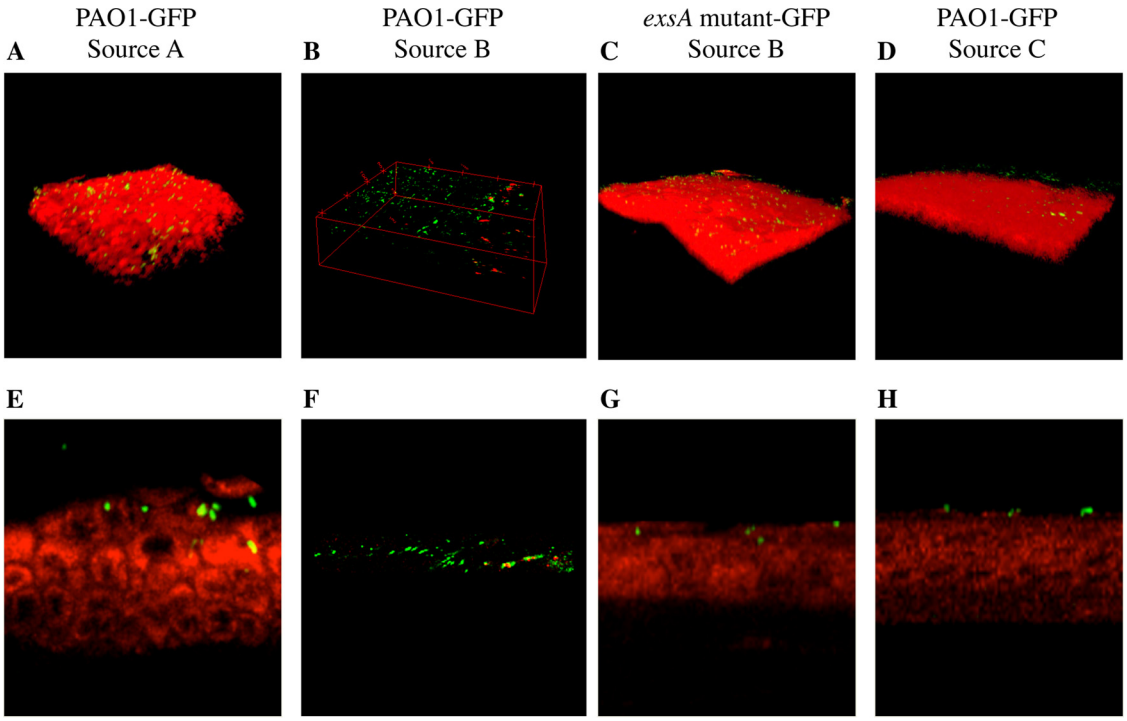

FIG 2 Three-dimensional images (A to D) and cross-sectional images (E to H) comparing three variants of *P. aeruginosa* strain PAO1-GFP and an *exsA* mutant (PAO1*exsA*::Ω-GFP) for their interaction with tissue paper-blotted and EGTA-treated (100 mM in PBS, 1 h) murine corneal epithelium *ex vivo*. (A and E) After 6 h, PAO1-GFP source A (46, 47) adhered to and partially traversed the corneal epithelium, which remained intact. (B and F) PAO1-GFP source B caused nearly complete loss of the corneal epithelium (as shown in Fig. 1). (C and G) The *exsA* mutant of strain PAO1-GFP source B showed binding but no traversal (as shown in Fig. 1). (D and H) PAO1-GFP source C showed binding to the murine corneal epithelium but no traversal, and the epithelium remained intact. Representative images from three independent experiments are shown. A Zeiss LSM 512 Meta W Plan-Apochromat (63×/1.0) objective lens was used. Images were acquired by confocal and 2-photon microscopy. Green, PAO1-GFP; red, epithelial cell autofluorescence.

the corneal epithelium, which remained relatively intact (Fig. 2A and E). The greater destruction of the corneal epithelium by PAO1 source B was evident (Fig. 2B and F [transverse section]). This bacterium-mediated damage was absent in the *exsA* (T3SS) mutant (Fig. 2C [experiment whose results are shown in Fig. 1B]), and transverse sections showed little or no bacterial traversal by the *exsA* mutant (Fig. 2G). In contrast, 6 h exposure to PAO1 source C caused little or no damage to the corneal epithelium, and bacteria adhered without penetrating the epithelium (Fig. 2D and H).

Quantitative measurements of corneal epithelial thickness (Fig. 3A) and bacterial traversal of the epithelium (Fig. 3B) after 6 h bacterial exposure were consistent with the images shown in Fig. 1 and 2. Corneal epithelial thickness data from Fig. 1E for PAO1 source B and its *exsA* mutant were included in Fig. 3A for comparison. Exposure to PAO1 source A and PAO1 source C for 6 h left the corneal epithelium at a thickness similar to that of the *exsA* mutant of PAO1 source B, and although these groups were not significantly different from each other, they were all significantly different from the PAO1 source B group ($P < 0.05$; ANOVA). Indeed, while epithelial thickness was lower in all bacterium-treated groups, only PAO1 source B-treated corneal epithelium was significantly different from uninoculated corneal epithelium with or without blotting and EGTA treatment (Fig. 3A). PAO1 source A showed greater traversal than PAO1 source C and the *exsA* mutant of PAO1 source B, but these groups were not significantly different from each other (Fig. 3B). PAO1 source B showed significantly greater traversal than its *exsA* mutant and PAO1 source C ($P < 0.05$; ANOVA) (Fig. 3B).

Quantification of *exsA* gene expression under T3SS-inducing conditions *in vitro* by RT-PCR (Fig. 4) showed a positive correlation with epithelial traversal by *P. aeruginosa ex vivo*. PAO1 sources A and B both displayed significant induction of *exsA* gene expression *in vitro* under T3SS-inducing conditions relative to noninducing conditions (Fig. 4). However, PAO1 source C yielded little or no induction of *exsA* gene expression, consistent with the lack of epithelial traversal and/or damage *ex vivo*.

Traversal of MyD88$^{-/-}$ mouse corneal epithelium is independent of ExsA. Another way we enabled *P. aeruginosa* to traverse the corneal epithelium involved the use of MyD88$^{-/-}$ mice (47). In this case, there is no need to blot or to EGTA treat the eye, as *P. aeruginosa* can adhere to and penetrate the intact untreated epithelium. Here, we tested the hypothesis that ExsA would also be required for *P. aeruginosa* to traverse MyD88$^{-/-}$ mouse corneal epithelium.

As expected wild-type PAO1-GFP source B (green) caused significant damage to the corneal epithelium of MyD88$^{-/-}$ mice, as indicated by complete loss of epithelial cell autofluorescence (red) (Fig. 5A). What was not expected was that the *exsA* (T3SS) mutant of *P. aeruginosa* PAO1 source B caused a similar amount of damage to the MyD88$^{-/-}$ epithelium (Fig. 5B), showing that ExsA was not required for bacteria traversal/damage in the case of MyD88 deficiency. Another difference between MyD88 deficiency and blotting-EGTA treatment was results obtained with PAO1 source

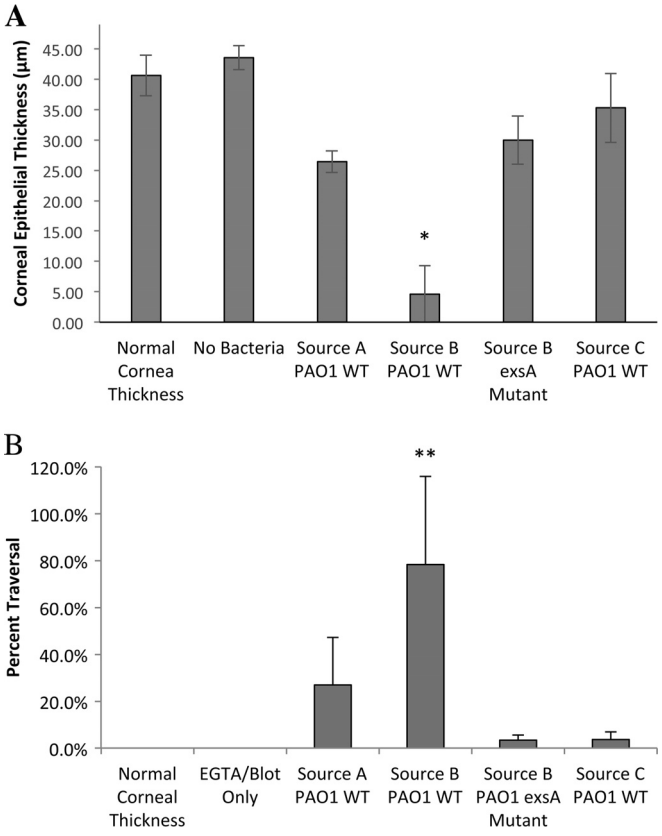

FIG 3 (A) Murine corneal epithelial thickness and (B) percentage epithelial traversal after 6 h exposure to three different sources of *P. aeruginosa* strain PAO1-GFP and an *exsA* mutant of PAO1-GFP source B (Fig. 1 and 2). Uninoculated controls included normal murine corneal epithelium and tissue paper-blotted and EGTA-treated (100 mM in PBS, 1 h) murine corneal epithelium. Data are means ± SD from three independent experiments. PAO1 source B and its *exsA* mutant data from Fig. 1E and F are shown in panels A and B, respectively, for comparison purposes. The single asterisk indicates a significant difference versus uninoculated corneas (normal cornea thickness), tissue paper-blotted and EGTA-treated corneas (no bacteria), and other bacterium-inoculated corneas ($P < 0.05$; ANOVA with Tukey's multiple-comparison *post hoc* analysis). The double asterisk indicates a significant difference versus traversal of *exsA* mutant and PAO1-GFP source C ($P < 0.05$; ANOVA with Tukey's multiple-comparison *post hoc* analysis).

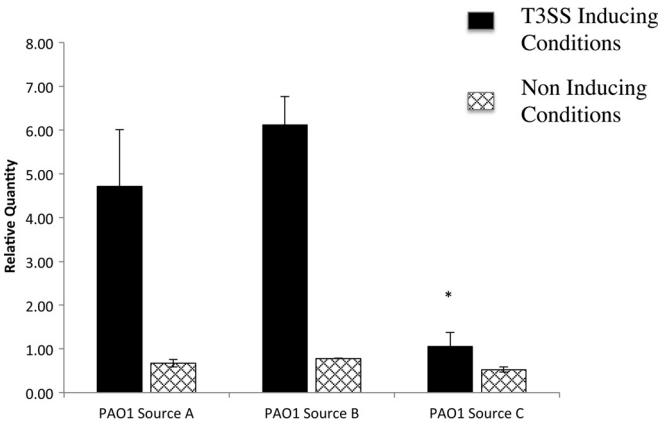

FIG 4 RT-PCR of *exsA* gene expression in three different sources of *P. aeruginosa* strain PAO1-GFP under T3SS-inducing conditions *in vitro* (see Materials and Methods) compared to noninducing conditions. PAO1-GFP source C showed significantly reduced T3SS induction compared to source B (*, $P < 0.05$; ANOVA with Tukey's multiple-comparison *post hoc* analysis). Results from one of two independent experiments are shown.

C. As discussed above, wild-type PAO1-GFP source C was unable to traverse the epithelium even after blotting-EGTA treatment. However, it was able to traverse the epithelium in MyD88$^{-/-}$ mice, even without blotting-ETGA treatment. This traversal left the epithelium relatively intact (Fig. 5C). As expected, control corneas of MyD88$^{-/-}$ mice appeared healthy and intact in the absence of bacterial inoculation (Fig. 5D). Exposure to PAO1 source C did not significantly affect epithelial thickness of MyD88$^{-/-}$ corneas (Fig. 5E), and bacterial traversal was evident throughout the corneal epithelium (Fig. 5F).

MyD88$^{-/-}$ corneal epithelium has reduced antimicrobial activity against *P. aeruginosa*. The susceptibility of MyD88$^{-/-}$ corneas to ExsA-independent traversal led us to investigate if MyD88 deficiency impaired antimicrobial activity of the corneal epithelium. Our choice to focus on antimicrobial activity, rather than other potential defense factors, was based on our earlier discoveries that corneally expressed antimicrobials (including mBD3 and keratin-derived antimicrobial peptides [KDAMPs]) contribute to maintaining the corneal epithelial barrier against *P. aeruginosa* (49, 59). Thus, the corneal epithelium of normal healthy wild-type and MyD88$^{-/-}$ mice was homogenized, and crude lysates were fractionated by molecular weight prior to bactericidal activity screening against *P. aeruginosa*. We observed that the 10- to 100-kDa and the <10-kDa lysate fractions of untreated wild-type but not MyD88 knockout mice retarded growth of *P. aeruginosa* (Fig. 6A) ($P < 0.0001$ and $P = 0.005$, respectively; *t* test), showing that MyD88 is critical for constitutive antimicrobial activity of the cornea. This activity was concentration dependent, since it was reduced or eliminated after 2-fold dilution of the ~10- to 100-kDa and <10-kDa wild-type corneal lysate fractions, respectively (Fig. 6A).

After exposure to *P. aeruginosa* antigens, the wild-type <10-kDa fraction remained antibacterial, while the activities of the 10- to 30-kDa and the 30- to 100-kDa fractions were magnified (Fig. 6B). In addition, the <10-kDa and the 10- to 30-kDa fractions from MyD88$^{-/-}$ mice also became antimicrobial (Fig. 6B), indicating that MyD88-independent pathways also contribute to antigen-activated antimicrobial activity. Nevertheless, all three corneal lysate fractions (30 to 100 kDa, 10 to 30 kDa, and <10 kDa) from antigen-challenged wild-type mice showed significantly more antibacterial activity than those derived from MyD88$^{-/-}$ mice (Fig. 6B) ($P < 0.05$, *t* test).

Analysis of corneal lysates by mass spectrometry. To begin to investigate potential determinants for the observed differences in antimicrobial activity between murine corneal lysates, we performed mass spectrometry on the 30- to 100-kDa corneal lysate fractions, which showed the greatest reduction in antimicrobial activity in MyD88$^{-/-}$ mice compared to wild-type mice (Fig. 6). Figure 7 shows that 120 different proteins were detectable only in unstimulated wild-type corneal lysates and not in the knockout (Fig. 7A). Similarly, 46 proteins were specific to wild-type-antigen-stimulated corneas compared to the knockout (Fig. 7B). Among the proteins shared between wild-type and knockout mice, 29 were more abundant under wild-type unstimulated conditions and 21 upon antigen stimulation (Fig. 7A and B). Proteins that were present or more abundant only in the wild-type corneal

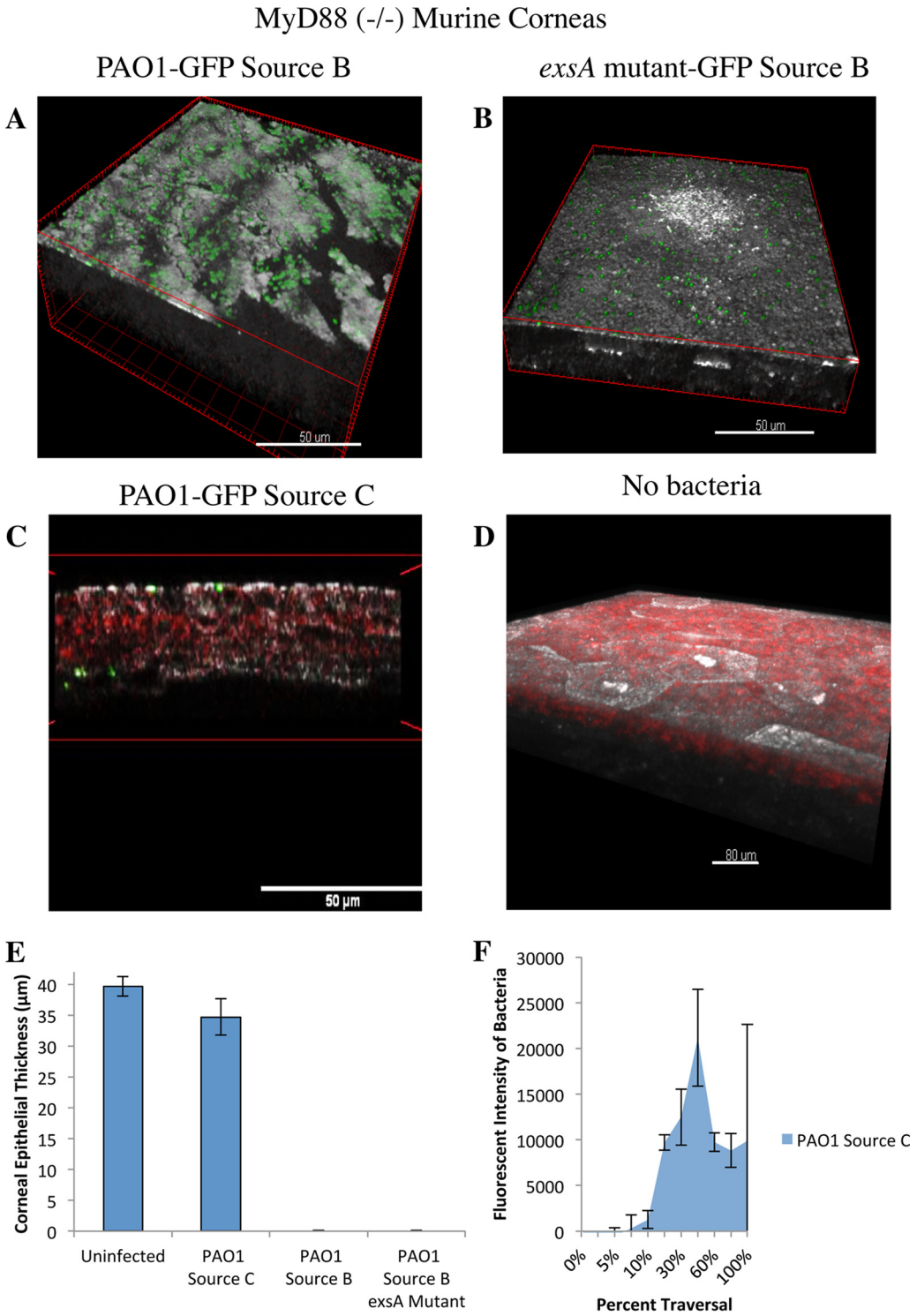

FIG 5 *P. aeruginosa* traversal of MyD88$^{-/-}$ murine corneal epithelium without prior tissue paper blotting or EGTA treatment. After exposure to *P. aeruginosa* strain PAO1-GFP source B (A) or its *exsA* mutant (PAO1*exsA*::Ω-GFP) (B), the corneas of MyD88$^{-/-}$ mice showed extensive and equivalent binding of wild-type and *exsA* mutant bacteria (green), with both causing significant damage to the murine corneal epithelium, as indicated by the absence of epithelial cell autofluorescence (red), determined by confocal and 2-photon microscopy. In panels A and B, reflectance (white) indicates the corneal stroma. Images are representative of three independent experiments. A Zeiss LSM 512 Meta W Plan-Apochromat (63×/1.0) objective lens was used. (C) *P. aeruginosa* strain PAO1-GFP source C (green) traversed the corneal epithelium of MyD88$^{-/-}$ mice after 6 h. (D) Control showing the MyD88$^{-/-}$ cornea without bacterial inoculation. In panels C and D, the epithelium remained intact, as indicated by epithelial cell autofluorescence (red). Images are representative of two independent experiments. (E and F) Murine corneal epithelial thickness (E) and percent epithelial traversal (F) for MyD88$^{-/-}$ corneas 6 h after exposure to PAO1-GFP source C compared to uninoculated controls.

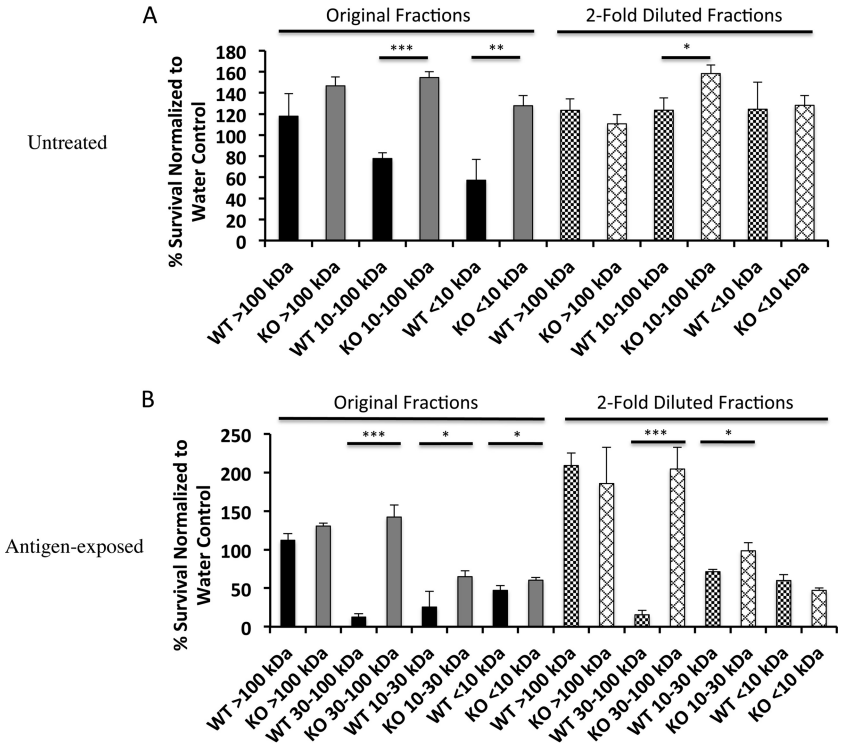

FIG 6 Antimicrobial activity of untreated (A) and antigen-exposed (B) wild-type (WT) and MyD88$^{-/-}$ (KO) mouse corneal lysate fractions. (A) Under normal healthy conditions, the 10- to 100-kDa and the <10-kDa fractions of wild-type but not MyD88-deficient mice inhibited the growth of *P. aeruginosa*. This activity was reduced or eliminated by 2-fold dilution of the fractions. (B) After exposure to *P. aeruginosa* antigens, the <10-kDa fractions of both wild-type and MyD88$^{-/-}$ mice were antipseudomonal. In addition, the antibacterial activities of the 30- to 100-kDa and the 10- to 30-kDa fractions of wild-type mice postinoculation were increased compared to that of 10- to 100-kDa fraction preinoculation. Means ± SD are shown. *, $P < 0.05$; **, $P < 0.01$; ***, $P < 0.001$ (*t* test).

lysates could account for the antimicrobial activity observed in this fraction both with and without bacterial antigen stimulation (Fig. 6A and B). Of interest, we found that (i) histones (H2a and H2b) and tubulin (alpha and beta subunits) were more abundant in unstimulated wild-type corneas than in MyD88$^{-/-}$ corneas and (ii) glutathione *S*-transferase and annexin were both more abundant in antigen-stimulated wild-type corneas. When we compared antigen-stimulated and unstimulated wild-type corneas, we

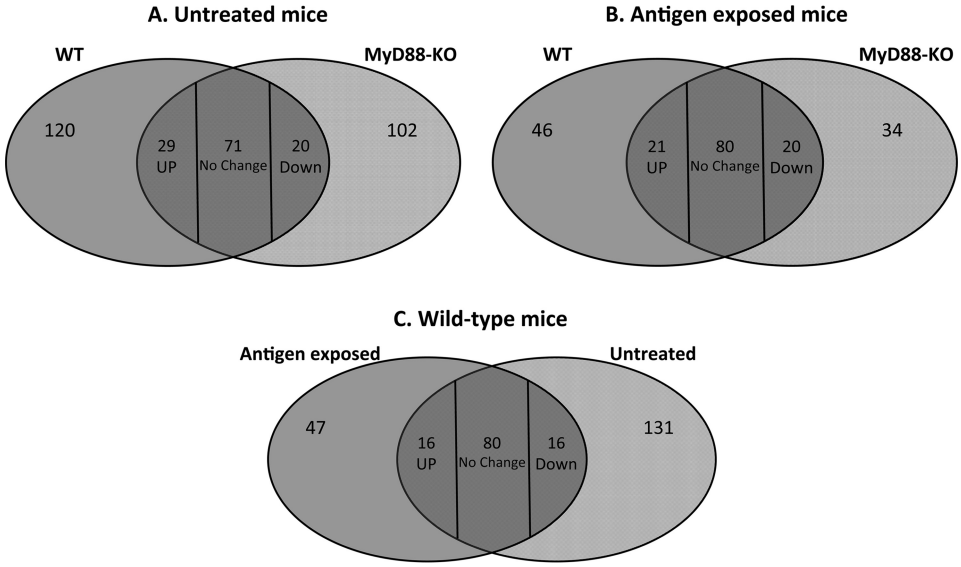

FIG 7 Venn diagrams showing comparison of protein content in the 30- to 100-kDa fraction of the corneal lysates. (A and B) Wild-type and MyD88$^{-/-}$ mice under normal healthy conditions without antigen challenge (A) and after antigen exposure (B). (C) Baseline versus antigen-activated expression in the wild-type mice. Numbers in each intersection represent proteins present in both categories that are up- or downregulated in the wild-type (A and B) or in the stimulated condition (C).

TABLE 1 Summary of findings regarding the relationship between *P. aeruginosa* traversal of the murine corneal epithelium *ex vivo* and expression of the T3SS in the presence and absence of MyD88

Mouse ocular genotype *ex vivo*	Pretreatment	*exsA* expression	Traversal
C57BL/6	Blotting-EGTA	Yes	Yes
C57BL/6	Blotting-EGTA	No	No
C57BL/6	Blotting-EGTA	High level	Yes
C57BL/6	Blotting-EGTA	Low level	No
C57BL/6 *myd88*$^{-/-}$	None	Yes	Yes
C57BL/6 *myd88*$^{-/-}$	None	No	Yes

found 63 protein species (47 + 16) present or more abundant only in the antigen-stimulated condition (Fig. 7C). These proteins are candidates for participation in the observed increase in antimicrobial activity of the wild-type corneas when stimulated with bacterial antigens.

The full list of proteins detected in the 30- to 100-kDa corneal lysate fractions and their relative abundance between wild-type and MyD88$^{-/-}$ mice and with and without antigen stimulation is presented in Fig. S1 in the supplemental material. In addition to the proteins mentioned above, two other groups of proteins (boxes in Fig. S1) were of interest: (i) nine proteins that were more abundant in *P. aeruginosa* antigen-challenged wild-type corneas than in antigen-challenged MyD88$^{-/-}$ corneas or in either type of untreated cornea, i.e., antigen upregulated and MyD88 dependent (blue box) (e.g., dermatopontin), and (ii) four proteins that were more abundant in wild-type than MyD88$^{-/-}$ corneas with and without antigen challenge, i.e., constitutively present (black box) (e.g., lumican).

DISCUSSION

In this study, we explored the role of the transcriptional activator ExsA, a regulator of the *P. aeruginosa* T3SS (58, 60), in epithelial traversal by the invasive *P. aeruginosa* strain PAO1 using multiple methods. For this, we used imaging and analysis strategies which we developed specifically for the purpose of studying bacterial traversal through the corneal epithelium of intact live mouse eyeballs (47). These methods allow the exact location of individual bacteria to be accurately determined while the topography of the cornea is monitored, yielding quantifiable data related to both features. This study was done utilizing unfixed and unlabeled whole live eyeballs but *ex vivo* to exclude extracorneal *in vivo* factors at the time of bacteria inoculation, thereby preventing them from confounding the outcome.

For corneas superficially injured by tissue paper blotting and subsequent EGTA treatment, we found that *P. aeruginosa* invasive strain PAO1 required ExsA to traverse the epithelium. This was shown using *exsA* mutants and was supported by a correlation found between *exsA* gene expression and the capacity for epithelial traversal for three separate isolates of PAO1 obtained from different sources. In stark contrast, *P. aeruginosa* remained able to traverse the corneal epithelium of MyD88-deficient mice independently of ExsA, even in the absence of any type of injury or treatment. A summary of these findings is shown in Table 1.

Given that ExsA is a transcriptional activator of the *P. aeruginosa* T3SS, the data suggested that the T3SS is required for invasive *P. aeruginosa* strain PAO1 to traverse the mouse corneal epithelium in the context of superficial epithelial injury involving tissue paper blotting and EGTA treatment but not in the context of immunocompromise relevant to MyD88 deficiency. Results obtained using the blotting-EGTA method also contrasted with our published findings obtained using the 6-h healing model discussed above, in which we found no role for ExsA in corneal entry into the stroma when the same invasive strain (PAO1) penetrated both healing corneal epithelium and basal lamina after scratching (45). Thus, the role of ExsA (and presumably the T3SS) in traversal of corneal epithelium by invasive *P. aeruginosa* is conditional upon the nature of epithelial compromise. Whether the role of ExsA/T3SS is conditional for other epithelium-lined tissue surfaces will need to be determined. Further studies will also be needed to pinpoint which T3SS effectors expressed by *P. aeruginosa* are involved in corneal epithelial traversal *in vivo* or *ex vivo* in situations where ExsA is required and for determining other invasive *P. aeruginosa* strain virulence factors contributing to traversal when ExsA is not needed. Candidate ExsA-independent factors driving epithelial traversal include various virulence factors shown to be involved in passaging through cultured cells, such as proteases, rhamnolipids, exotoxin A, and the MexAB/OprM antimicrobial efflux pump (27, 38, 39, 41, 61). Whatever the case, ExsA-independent factors driving traversal could differ in the 6-h healing corneas and MyD88-compromised corneas considering that (i) the barrier function with regard to fluorescein is lost in the former (45) but not in the latter (47) situation and (ii) that MyD88-deficient epithelia are defective in expression of many defense factors (51, 52, 62, 63), including those identified in this study.

Obvious candidate mechanisms for why MyD88 deficiency allows *P. aeruginosa* to penetrate the corneal epithelial barrier even when the bacteria lack their T3SS include defects in junctional integrity or expression of antimicrobial peptides. However, epithelial barrier function with regard to the small molecule fluorescein remains intact in the corneas of MyD88-deficient mice (47), making the former unlikely. Since we had found that antimicrobial peptides can contribute to defense against epithelial traversal in the cornea (49, 59), we explored antimicrobial activity of MyD88$^{-/-}$ corneal epithelium and found that it was reduced compared to that in wild-type mice, both with and without antigenic challenge.

Differences in antimicrobial activities of corneal epithelial cell lysates between wild-type and MyD88$^{-/-}$ corneas were greatest in the 30- to 100-kDa lysate fractions, especially after antigenic challenge, suggesting that factors involved were both constitutively expressed and inducible. Interestingly, differences in protein content without antigen stimulation in this fraction included histones 2A and 2B. Histone 2A is a known precursor of a potent antimicrobial peptide, e.g., parasin I (19-mer), which is generated in the wounded skin mucosa of catfish by cathepsin D (64), and the related peptide hipposin (51-mer), which is found in the skin mucus of Atlantic halibut (65). Thus, there is good evidence that histone-derived antimicrobials can participate in host defense (66). Interestingly, lumican was less abundant in MyD88$^{-/-}$ samples with and without antigen stimulation. This extracellular matrix protein was previously shown to be important for Toll-like receptor 4 (TLR 4)-mediated proinflammatory responses to lipopolysaccharide (67) and clearance of *P. aeruginosa* from infected murine corneas (68). Our data suggest that lumican is also regulated by MyD88 in the murine cornea. Also intriguing was that antigen-challenged MyD88$^{-/-}$ corneas expressed significantly

less glutathione *S*-transferase than wild-type corneas. Previous studies have shown increased susceptibility to bacterial infection in glutathione *S*-transferase gene knockout mice (mGSTA4-4) (69), and GST2 gene knockout *Drosophila* organisms display increased susceptibility to *P. aeruginosa* infection (19). Thermal injury, which increases susceptibility to *P. aeruginosa* infection, decreases hGSTA4 expression in humans and mGSTA4 in mice (70). Further, glutathione is associated with antimicrobial activity against *Mycobacterium tuberculosis* in macrophages (71). Finally, dermatopontin, another extracellular matrix protein, was also less abundant in MyD88$^{-/-}$ corneas after antigen challenge and at baseline in both wild-type and MyD88$^{-/-}$ corneas. The dermatopontin gene was upregulated 900-fold after *Vibrio parahaemolyticus* challenge in an invertebrate model (72), and the protein was shown to promote keratinocyte migration (73), which is important for re-epithelialization during wound healing. Future studies will explore the involvement of these potentially interesting factors impacted by MyD88 deficiency (and others listed in Fig. S1 in the supplemental material), in both constitutive and activated defense of the corneal epithelium.

The capacity of PAO1 and other *P. aeruginosa* strains to advance their fitness to adapt to different environments has been well documented and has been shown to be due to both general and inducible hypermutation (74). The intrastrain variability in T3SS expression *in vitro* between *P. aeruginosa* PAO1 sources A, B, and C and correlated major differences in how they interacted with the epithelium found in this study provide a functional example. This highlights the importance of using appropriate parental wild-type bacteria when mutants are used to study bacterial pathogenesis. It also raises concerns about comparing studies between laboratories and potentially even in the same laboratory over time.

In conclusion, the data presented in this study show that a single invasive *P. aeruginosa* isolate can use multiple mechanisms for traversing the corneal epithelium conditional on the nature of host susceptibility. Some forms of superficial injury can promote ExsA-dependent traversal, which likely involves one or more T3SS effectors, while immunocompromise caused by MyD88 deficiency can make the T3SS dispensable for penetrating an epithelial multilayer, even when barrier function with regard to the small molecule fluorescein remains intact. The fact that multiple virulence factors can allow one strain to penetrate protective epithelial barriers suggests that strategies that target only one virulence determinant (e.g., the T3SS) might not be effective under all circumstances. The data also question the value of using immunocompetent animal models for studying infections associated with immunocompromise.

Contact lens wear is the most common cause of corneal infection caused by *P. aeruginosa* and has the potential to suppress MyD88-modulated defenses, at least in cultured cells (56). Further, lens wear can also cause superficial epithelial defects (75, 76), while lens care products can contain calcium chelators similar to EGTA (77). Whether any of the models or results obtained with them presented here relate directly to why or how *P. aeruginosa* sometimes penetrates the corneal epithelium during contact lens wear remains to be determined.

ACKNOWLEDGMENTS

This work was supported by the National Eye Institute (EY011221 to S.M.J.F. and EY023000 to K.P.C.T.).

We express our thanks to Dara Frank (Medical College of Wisconsin), Gerald Pier (Harvard Medical School), Arne Rietsch (Case Western Reserve University), and Timothy Yahr (University of Iowa) for providing *P. aeruginosa* wild-type strains, mutants, and plasmid constructs used in this study and to Lori Kohlstaedt (Proteomics/Mass Spectrometry Laboratory, University of California, Berkeley) for instrumentation and helpful advice.

Suzanne M. J. Fleiszig is a paid consultant for Allergan Inc. Irvine, CA, USA. However, that work is unrelated to the content of this study.

REFERENCES

1. **Chalmers JD, Rother C, Salih W, Ewig S.** 2014. Healthcare-associated pneumonia does not accurately identify potentially resistant pathogens: a systematic review and meta-analysis. Clin Infect Dis **58:**330–339. http://dx.doi.org/10.1093/cid/cit734.
2. **Azzopardi EA, Azzopardi E, Camilleri L, Villapalos J, Boyce DE, Dziewulski P, Dickson WA, Whitaker IS.** 2014. Gram negative wound infection in hospitalised adult burn patients-systematic review and metanalysis. PLoS One **9:**e95042. http://dx.doi.org/10.1371/journal.pone.0095042.
3. **Mikulska M, Viscoli C, Orasch C, Livermore DM, Averbuch D, Cordonnier C, Akova M.** 2014. Aetiology and resistance in bacteraemias among adult and paediatric haematology and cancer patients. J Infect **68:**321–331. http://dx.doi.org/10.1016/j.jinf.2013.12.006.
4. **Zilberberg MD, Shorr AF.** 2013. Secular trends in gram-negative resistance among urinary tract infection hospitalizations in the United States, 2000-2009. Infect Control Hosp Epidemiol **34:**940–946. http://dx.doi.org/10.1086/671740.
5. **Lichtinger A, Yeung SN, Kim P, Amiran MD, Iovieno A, Elbaz U, Ku JY, Wolff R, Rootman DS, Slomovic AR.** 2012. Shifting trends in bacterial keratitis in Toronto: an 11-year review. Ophthalmology **119:**1785–1790. http://dx.doi.org/10.1016/j.ophtha.2012.03.031.
6. **Yildiz EH, Airiani S, Hammersmith KM, Rapuano CJ, Laibson PR, Virdi AS, Hongyok T, Cohen EJ.** 2012. Trends in contact lens-related corneal ulcers at a tertiary referral center. Cornea **31:**1097–1102. http://dx.doi.org/10.1097/ICO.0b013e318221cee0.
7. **Fleiszig SM, Zaidi TS, Preston MJ, Grout M, Evans DJ, Pier GB.** 1996. Relationship between cytotoxicity and corneal epithelial cell invasion by clinical isolates of *Pseudomonas aeruginosa*. Infect Immun **64:**2288–2294.
8. **Angus AA, Evans DJ, Barbieri JT, Fleiszig SM.** 2010. The ADP-ribosylation domain of *Pseudomonas aeruginosa* ExoS is required for membrane bleb niche formation and bacterial survival within epithelial cells. Infect Immun **78:**4500–4510. http://dx.doi.org/10.1128/IAI.00417-10.
9. **Heimer SR, Evans DJ, Stern ME, Barbieri JT, Yahr T, Fleiszig SM.** 2013. *Pseudomonas aeruginosa* utilizes the type III secreted toxin ExoS to avoid acidified compartments within epithelial cells. PLoS One **8:**e73111. http://dx.doi.org/10.1371/journal.pone.0073111.
10. **Hritonenko V, Evans DJ, Fleiszig SM.** 2012. Translocon-independent intracellular replication by *Pseudomonas aeruginosa* requires the ADP-ribosylation domain of ExoS. Microbes Infect **14:**1366–1373. http://dx.doi.org/10.1016/j.micinf.2012.08.007.
11. **Fleiszig SM, Wiener-Kronish JP, Miyazaki H, Vallas V, Mostov KE, Kanada D, Sawa T, Yen TS, Frank DW.** 1997. *Pseudomonas aeruginosa*-mediated cytotoxicity and invasion correlate with distinct genotypes at the loci encoding exoenzyme S. Infect Immun **65:**579–586.
12. **Finck-Barbancon V, Goranson J, Zhu L, Sawa T, Wiener-Kronish JP, Fleiszig SM, Wu C, Mende-Mueller L, Frank DW.** 1997. ExoU expression by *Pseudomonas aeruginosa* correlates with acute cytotoxicity and epithelial injury. Mol Microbiol **25:**547–557. http://dx.doi.org/10.1046/j.1365-2958.1997.4891851.x.
13. **Pearlman E, Sun Y, Roy S, Karmakar M, Hise AG, Szczotka-Flynn L, Ghannoum M, Chinnery HR, McMenamin PG, Rietsch A.** 2013. Host defense at the ocular surface. Int Rev Immunol **32:**4–18. http://dx.doi.org/10.3109/08830185.2012.749400.
14. **Hauser AR.** 2009. The type III secretion system of *Pseudomonas aeruginosa*: infection by injection. Nat Rev Microbiol **7:**654–665. http://dx.doi.org/10.1038/nrmicro2199.
15. **Engel J, Balachandran P.** 2009. Role of *Pseudomonas aeruginosa* type III effectors in disease. Curr Opin Microbiol **12:**61–66. http://dx.doi.org/10.1016/j.mib.2008.12.007.
16. **Papaioannou E, Wahjudi M, Nadal-Jimenez P, Koch G, Setroikromo R, Quax WJ.** 2009. Quorum-quenching acylase reduces the virulence of *Pseudomonas aeruginosa* in a *Caenorhabditis elegans* infection model.

Antimicrob Agents Chemother **53:**4891–4897. http://dx.doi.org/10.1128/AAC.00380-09.
17. **Prithiviraj B, Bais HP, Weir T, Suresh B, Najarro EH, Dayakar BV, Schweizer HP, Vivanco JM.** 2005. Down regulation of virulence factors of *Pseudomonas aeruginosa* by salicylic acid attenuates its virulence on *Arabidopsis thaliana* and *Caenorhabditis elegans*. Infect Immun **73:**5319–5328. http://dx.doi.org/10.1128/IAI.73.9.5319-5328.2005.
18. **Adonizio A, Leal SM, Jr, Ausubel FM, Mathee K.** 2008. Attenuation of *Pseudomonas aeruginosa* virulence by medicinal plants in a *Caenorhabditis elegans* model system. J Med Microbiol **57:**809–813. http://dx.doi.org/10.1099/jmm.0.47802-0.
19. **Apidianakis Y, Mindrinos MN, Xiao W, Tegos GP, Papisov MI, Hamblin MR, Davis RW, Tompkins RG, Rahme LG.** 2007. Involvement of skeletal muscle gene regulatory network in susceptibility to wound infection following trauma. PLoS One **2:**e1356. http://dx.doi.org/10.1371/journal.pone.0001356.
20. **Balachandran P, Dragone L, Garrity-Ryan L, Lemus A, Weiss A, Engel J.** 2007. The ubiquitin ligase Cbl-b limits *Pseudomonas aeruginosa* exotoxin T-mediated virulence. J Clin Invest **117:**419–427. http://dx.doi.org/10.1172/JCI28792.
21. **Shaver CM, Hauser AR.** 2004. Relative contributions of *Pseudomonas aeruginosa* ExoU, ExoS, and ExoT to virulence in the lung. Infect Immun **72:**6969–6977. http://dx.doi.org/10.1128/IAI.72.12.6969-6977.2004.
22. **Vance RE, Rietsch A, Mekalanos JJ.** 2005. Role of the type III secreted exoenzymes S, T, and Y in systemic spread of *Pseudomonas aeruginosa* PAO1 in vivo. Infect Immun **73:**1706–1713. http://dx.doi.org/10.1128/IAI.73.3.1706-1713.2005.
23. **Holder IA, Wheeler R.** 1984. Experimental studies of the pathogenesis of infections owing to *Pseudomonas aeruginosa*: elastase, an IgG protease. Can J Microbiol **30:**1118–1124. http://dx.doi.org/10.1139/m84-175.
24. **Rumbaugh KP, Griswold JA, Iglewski BH, Hamood AN.** 1999. Contribution of quorum sensing to the virulence of *Pseudomonas aeruginosa* in burn wound infections. Infect Immun **67:**5854–5862.
25. **Turner KH, Everett J, Trivedi U, Rumbaugh KP, Whiteley M.** 2014. Requirements for *Pseudomonas aeruginosa* acute burn and chronic surgical wound infection. PLoS Genet **10:**e1004518. http://dx.doi.org/10.1371/journal.pgen.1004518.
26. **Koh AY, Mikkelsen PJ, Smith RS, Coggshall KT, Kamei A, Givskov M, Lory S, Pier GB.** 2010. Utility of in vivo transcription profiling for identifying *Pseudomonas aeruginosa* genes needed for gastrointestinal colonization and dissemination. PLoS One **5:**e15131. http://dx.doi.org/10.1371/journal.pone.0015131.
27. **Hirakata Y, Srikumar R, Poole K, Gotoh N, Suematsu T, Kohno S, Kamihira S, Hancock RE, Speert DP.** 2002. Multidrug efflux systems play an important role in the invasiveness of *Pseudomonas aeruginosa*. J Exp Med **196:**109–118. http://dx.doi.org/10.1084/jem.20020005.
28. **Lee EJ, Cowell BA, Evans DJ, Fleiszig SM.** 2003. Contribution of ExsA-regulated factors to corneal infection by cytotoxic and invasive *Pseudomonas aeruginosa* in a murine scarification model. Invest Ophthalmol Vis Sci **44:**3892–3898. http://dx.doi.org/10.1167/iovs.02-1302.
29. **Hazlett LD, Masinick S, Barrett R, Rosol K.** 1993. Evidence for asialo GM1 as a corneal glycolipid receptor for *Pseudomonas aeruginosa* adhesion. Infect Immun **61:**5164–5173.
30. **Tam C, Lewis SE, Li WY, Lee E, Evans DJ, Fleiszig SM.** 2007. Mutation of the phospholipase catalytic domain of the *Pseudomonas aeruginosa* cytotoxin ExoU abolishes colonization promoting activity and reduces corneal disease severity. Exp Eye Res **85:**799–805. http://dx.doi.org/10.1016/j.exer.2007.08.015.
31. **Hazlett LD, Zucker M, Berk RS.** 1992. Distribution and kinetics of the inflammatory cell response to ocular challenge with *Pseudomonas aeruginosa* in susceptible versus resistant mice. Ophthalmic Res **24:**32–39. http://dx.doi.org/10.1159/000267142.
32. **Hazlett LD, Berk RS.** 1984. Effect of C3 depletion on experimental *Pseudomonas aeruginosa* ocular infection: histopathological analysis. Infect Immun **43:**783–790.
33. **Wu M, Peng A, Sun M, Deng Q, Hazlett LD, Yuan J, Liu X, Gao Q, Feng L, He J, Zhang P, Huang X.** 2011. TREM-1 amplifies corneal inflammation after *Pseudomonas aeruginosa* infection by modulating Toll-like receptor signaling and Th1/Th2-type immune responses. Infect Immun **79:**2709–2716. http://dx.doi.org/10.1128/IAI.00144-11.
34. **Hazlett LD.** 2004. Corneal response to *Pseudomonas aeruginosa* infection. Prog Retin Eye Res **23:**1–30. http://dx.doi.org/10.1016/j.preteyeres.2003.10.002.
35. **Sun M, Zhu M, Chen K, Nie X, Deng Q, Hazlett LD, Wu Y, Li M, Wu M, Huang X.** 2013. TREM-2 promotes host resistance against *Pseudomonas aeruginosa* infection by suppressing corneal inflammation via a PI3K/Akt signaling pathway. Invest Ophthalmol Vis Sci **54:**3451–3462. http://dx.doi.org/10.1167/iovs.12-10938.
36. **Zolfaghar I, Evans DJ, Ronaghi R, Fleiszig SM.** 2006. Type III secretion-dependent modulation of innate immunity as one of multiple factors regulated by *Pseudomonas aeruginosa* RetS. Infect Immun **74:**3880–3889. http://dx.doi.org/10.1128/IAI.01891-05.
37. **Soong G, Parker D, Magargee M, Prince AS.** 2008. The type III toxins of *Pseudomonas aeruginosa* disrupt epithelial barrier function. J Bacteriol **190:**2814–2821. http://dx.doi.org/10.1128/JB.01567-07.
38. **Azghani AO, Gray LD, Johnson AR.** 1993. A bacterial protease perturbs the paracellular barrier function of transporting epithelial monolayers in culture. Infect Immun **61:**2681–2686.
39. **Azghani AO.** 1996. *Pseudomonas aeruginosa* and epithelial permeability: role of virulence factors elastase and exotoxin A. Am J Respir Cell Mol Biol **15:**132–140. http://dx.doi.org/10.1165/ajrcmb.15.1.8679217.
40. **Alarcon I, Evans DJ, Fleiszig SM.** 2009. The role of twitching motility in *Pseudomonas aeruginosa* exit from and translocation of corneal epithelial cells. Invest Ophthalmol Vis Sci **50:**2237–2244. http://dx.doi.org/10.1167/iovs.08-2785.
41. **Alarcon I, Kwan L, Yu C, Evans DJ, Fleiszig SM.** 2009. Role of the corneal epithelial basement membrane in ocular defense against *Pseudomonas aeruginosa*. Infect Immun **77:**3264–3271. http://dx.doi.org/10.1128/IAI.00111-09.
42. **Ramirez JC, Fleiszig SM, Sullivan AB, Tam C, Borazjani R, Evans DJ.** 2012. Traversal of multilayered corneal epithelia by cytotoxic *Pseudomonas aeruginosa* requires the phospholipase domain of exoU. Invest Ophthalmol Vis Sci **53:**448–453. http://dx.doi.org/10.1167/iovs.11-8999.
43. **Mun JJ, Tam C, Evans DJ, Fleiszig SM.** 2011. Modulation of epithelial immunity by mucosal fluid. Sci Rep **1:**8. http://dx.doi.org/10.1038/srep00008.
44. **Mun J, Tam C, Chan G, Kim JH, Evans D, Fleiszig S.** 2013. MicroRNA-762 is upregulated in human corneal epithelial cells in response to tear fluid and *Pseudomonas aeruginosa* antigens and negatively regulates the expression of host defense genes encoding RNase7 and ST2. PLoS One **8:**e57850. http://dx.doi.org/10.1371/journal.pone.0057850.
45. **Lee EJ, Evans DJ, Fleiszig SM.** 2003. Role of *Pseudomonas aeruginosa* ExsA in penetration through corneal epithelium in a novel in vivo model. Invest Ophthalmol Vis Sci **44:**5220–5227. http://dx.doi.org/10.1167/iovs.03-0229.
46. **Alarcon I, Tam C, Mun JJ, Ledue J, Evans DJ, Fleiszig SM.** 2011. Factors impacting corneal epithelial barrier function against *Pseudomonas aeruginosa* traversal. Invest Ophthalmol Vis Sci **52:**1368–1377. http://dx.doi.org/10.1167/iovs.10-6125.
47. **Tam C, Ledue J, Mun JJ, Herzmark P, Robey EA, Evans DJ, Fleiszig SM.** 2011. 3D quantitative imaging of unprocessed live tissue reveals epithelial defense against bacterial adhesion and subsequent traversal requires MyD88. PLoS One **6:**e24008. http://dx.doi.org/10.1371/journal.pone.0024008.
48. **Mun JJ, Tam C, Kowbel D, Hawgood S, Barnett MJ, Evans DJ, Fleiszig SM.** 2009. Clearance of *Pseudomonas aeruginosa* from a healthy ocular surface involves surfactant protein D and is compromised by bacterial elastase in a murine null-infection model. Infect Immun **77:**2392–2398. http://dx.doi.org/10.1128/IAI.00173-09.
49. **Augustin DK, Heimer SR, Tam C, Li WY, Le Due JM, Evans DJ, Fleiszig SM.** 2011. Role of defensins in corneal epithelial barrier function against *Pseudomonas aeruginosa* traversal. Infect Immun **79:**595–605. http://dx.doi.org/10.1128/IAI.00854-10.
50. **Hazlett LD, Wells PA, Berk RS.** 1984. Scanning electron microscopy of the normal and experimentally infected ocular surface. Scan Electron Microsc 1379–1389.
51. **Redfern RL, Reins RY, McDermott AM.** 2011. Toll-like receptor activation modulates antimicrobial peptide expression by ocular surface cells. Exp Eye Res **92:**209–220. http://dx.doi.org/10.1016/j.exer.2010.12.005.
52. **McDermott AM, Redfern RL, Zhang B, Pei Y, Huang L, Proske RJ.** 2003. Defensin expression by the cornea: multiple signalling pathways mediate IL-1beta stimulation of hBD-2 expression by human corneal epithelial cells. Invest Ophthalmol Vis Sci **44:**1859–1865. http://dx.doi.org/10.1167/iovs.02-0787.
53. **Frank DW, Nair G, Schweizer HP.** 1994. Construction and characterization of chromosomal insertional mutations of the *Pseudomonas aeruginosa* exoenzyme S trans-regulatory locus. Infect Immun **62:**554–563.
54. **Brutinel ED, Vakulskas CA, Brady KM, Yahr TL.** 2008. Characterization of ExsA and of ExsA-dependent promoters required for expression of the

Pseudomonas aeruginosa type III secretion system. Mol Microbiol **68:**657–671. http://dx.doi.org/10.1111/j.1365-2958.2008.06179.x.
55. **Yahr TL, Mende-Mueller LM, Friese MB, Frank DW.** 1997. Identification of type III secreted products of the *Pseudomonas aeruginosa* exoenzyme S regulon. J Bacteriol **179:**7165–7168.
56. **Maltseva IA, Fleiszig SM, Evans DJ, Kerr S, Sidhu SS, McNamara NA, Basbaum C.** 2007. Exposure of human corneal epithelial cells to contact lenses in vitro suppresses the upregulation of human beta-defensin-2 in response to antigens of *Pseudomonas aeruginosa*. Exp Eye Res **85:**142–153. http://dx.doi.org/10.1016/j.exer.2007.04.001.
57. **Liu H, Sadygov RG, Yates JR, III.** 2004. A model for random sampling and estimation of relative protein abundance in shotgun proteomics. Anal Chem **76:**4193–4201. http://dx.doi.org/10.1021/ac0498563.
58. **Yahr TL, Frank DW.** 1994. Transcriptional organization of the trans-regulatory locus which controls exoenzyme S synthesis in *Pseudomonas aeruginosa*. J Bacteriol **176:**3832–3838.
59. **Tam C, Mun JJ, Evans DJ, Fleiszig SM.** 2012. Cytokeratins mediate epithelial innate defense through their antimicrobial properties. J Clin Invest **122:**3665–3677. http://dx.doi.org/10.1172/JCI64416.
60. **Brutinel ED, Vakulskas CA, Yahr TL.** 2009. Functional domains of ExsA, the transcriptional activator of the *Pseudomonas aeruginosa* type III secretion system. J Bacteriol **191:**3811–3821. http://dx.doi.org/10.1128/JB.00002-09.
61. **Wallace CJ, Medina SH, Elsayed ME.** 2014. Effect of rhamnolipids on permeability across Caco-2 cell monolayers. Pharm Res **31:**887–894. http://dx.doi.org/10.1007/s11095-013-1210-5.
62. **Kumar A, Yin J, Zhang J, Yu FS.** 2007. Modulation of corneal epithelial innate immune response to *Pseudomonas* infection by flagellin pretreatment. Invest Ophthalmol Vis Sci **48:**4664–4670. http://dx.doi.org/10.1167/iovs.07-0473.
63. **Kumar A, Zhang J, Yu FS.** 2006. Toll-like receptor 2-mediated expression of beta-defensin-2 in human corneal epithelial cells. Microbes Infect **8:**380–389. http://dx.doi.org/10.1016/j.micinf.2005.07.006.
64. **Cho JH, Park IY, Kim HS, Lee WT, Kim MS, Kim SC.** 2002. Cathepsin D produces antimicrobial peptide parasin I from histone H2A in the skin mucosa of fish. FASEB J **16:**429–431. http://dx.doi.org/10.1096/fj.01-0736fje.
65. **Birkemo GA, Luders T, Andersen O, Nes IF, Nissen-Meyer J.** 2003. Hipposin, a histone-derived antimicrobial peptide in Atlantic halibut (*Hippoglossus hippoglossus L.*). Biochim Biophys Acta **1646:**207–215. http://dx.doi.org/10.1016/S1570-9639(03)00018-9.
66. **Kawasaki H, Iwamuro S.** 2008. Potential roles of histones in host defense as antimicrobial agents. Infect Disord Drug Targets **8:**195–205. http://dx.doi.org/10.2174/187152651080803019 5.
67. **Wu F, Vij N, Roberts L, Lopez-Briones S, Joyce S, Chakravarti S.** 2007. A novel role of the lumican core protein in bacterial lipopolysaccharide-induced innate immune response. J Biol Chem **282:**26409–26417. http://dx.doi.org/10.1074/jbc.M702402200.
68. **Shao H, Scott SG, Nakata C, Hamad AR, Chakravarti S.** 2013. Extracellular matrix protein lumican promotes clearance and resolution of *Pseudomonas aeruginosa* keratitis in a mouse model. PLoS One **8:**e54765. http://dx.doi.org/10.1371/journal.pone.0054765.
69. **Engle MR, Singh SP, Czernik PJ, Gaddy D, Montague DC, Ceci JD, Yang Y, Awasthi S, Awasthi YC, Zimniak P.** 2004. Physiological role of mGSTA4-4, a glutathione S-transferase metabolizing 4-hydroxynonenal: generation and analysis of mGsta4 null mouse. Toxicol Appl Pharmacol **194:**296–308. http://dx.doi.org/10.1016/j.taap.2003.10.001.
70. **Apidianakis Y, Que YA, Xu W, Tegos GP, Zimniak P, Hamblin MR, Tompkins RG, Xiao W, Rahme LG.** 2012. Down-regulation of glutatione S-transferase alpha 4 (hGSTA4) in the muscle of thermally injured patients is indicative of susceptibility to bacterial infection. FASEB J **26:**730–737. http://dx.doi.org/10.1096/fj.11-192484.
71. **Morris D, Khurasany M, Nguyen T, Kim J, Guilford F, Mehta R, Gray D, Saviola B, Venketaraman V.** 2013. Glutathione and infection. Biochim Biophys Acta **1830:**3329–3349. http://dx.doi.org/10.1016/j.bbagen.2012.10.012.
72. **Huang G, Liu H, Han Y, Fan L, Zhang Q, Liu J, Yu X, Zhang L, Chen S, Dong M, Wang L, Xu A.** 2007. Profile of acute immune response in Chinese amphioxus upon *Staphylococcus aureus* and *Vibrio parahaemolyticus* infection. Dev Comp Immunol **31:**1013–1023. http://dx.doi.org/10.1016/j.dci.2007.01.003.
73. **Krishnaswamy VR, Korrapati PS.** 2014. Role of dermatopontin in re-epithelialization: implications on keratinocyte migration and proliferation. Sci Rep **4:**7385. http://dx.doi.org/10.1038/srep07385.
74. **Weigand MR, Sundin GW.** 2012. General and inducible hypermutation facilitate parallel adaptation in *Pseudomonas aeruginosa* despite divergent mutation spectra. Proc Natl Acad Sci U S A **109:**13680–13685. http://dx.doi.org/10.1073/pnas.1205357109.
75. **Ichijima H, Yokoi N, Nishizawa A, Kinoshita S.** 1999. Fluorophotometric assessment of rabbit corneal epithelial barrier function after rigid contact lens wear. Cornea **18:**87–91. http://dx.doi.org/10.1097/00003226-199901000-00015.
76. **McNamara NA, Polse KA, Fukunaga SA, Maebori JS, Suzuki RM.** 1998. Soft lens extended wear affects epithelial barrier function. Ophthalmology **105:**2330–2335. http://dx.doi.org/10.1016/S0161-6420(98)91237-4.
77. **Gorbet MB, Tanti NC, Crockett B, Mansour L, Jones L.** 2011. Effect of contact lens material on cytotoxicity potential of multipurpose solutions using human corneal epithelial cells. Mol Vis **17:**3458–3467. http://dx.doi.org/10.1371/journal.pone.0096448.